JOURNAL OF MATERIALS SCIENCE **39** (2004) 1283–1295

Crack toughness behavior of binary poly(styrene-butadiene) block copolymer blends

R. LACH, R. ADHIKARI
Institute of Materials Science, Martin-Luther University Halle-Wittenberg, D-06099 Halle/Saale, Germany

R. WEIDISCH*
Institute of Polymer Research Dresden, Hohe Straße 6, D-01069 Dresden, Germany
E-mail: weidisch@ipfdd.de

T. A. HUY, G. H. MICHLER, W. GRELLMANN
Institute of Materials Science, Martin-Luther University Halle-Wittenberg, D-06099 Halle/Saale, Germany

K. KNOLL
BASF AG, Polymer Research Laboratory, ZKT/I-B1, D-67056 Ludwigshafen, Germany

Fracture behavior of binary blends comprising styrene-butadiene block copolymers having star and triblock architectures was studied by instrumented Charpy impact test. The toughness of the ductile blends was characterized by the dynamic crack resistance concept (*R* curves). While the lamellar thermoplastic star block copolymer shows elastic behavior (small scale yielding and unstable crack growth), adding 20 wt% of a triblock copolymer (thermoplastic elastomer, TPE) leads to a strong increase in crack toughness. The stable crack propagation behavior of these blends was described by the crack resistance curve (*R*) concept of elastic-plastic fracture mechanics. This concept allows the determination of fracture mechanics parameters as resistance against stable crack initiation and propagation. Two brittle to tough transitions (BTT) are observed in the binary block copolymer blend: BTT1 at 20% TPE and BTT2 at about 60% TPE. The strong increase of toughness at 60 wt% TPE indicates a 'tough/high-impact' transition as a measure for the protection against stable crack initiation.

The kinetics of stable crack propagation is discussed with respect to deformation mechanisms and crack-tip blunting behavior. The analysis of fracture surface by SEM revealed three different types of deformation mechanisms depending on the weight fraction of TPE: coalescence of microvoids (similar to semicrystalline polymers), shear flow (typical of many amorphous polymers like polycarbonate) and tearing (similar to elastomers). Our investigations on nanostructured binary block copolymer blends show new possibilities to tailor the toughness of polymer materials associated with complex morphology-toughness correlations. This may lead to new materials concepts for toughened nanostructured polymers, which still maintain excellent transparency.

1. Introduction

Block copolymers represent a special class of self-assembled nanostructured materials, the structure and size of whose morphology can be controlled by molecular architecture, molecular weight, and composition. Self-assembled materials provide a versatile tool to create desired nanostructures in bulk materials or at interfaces, which have potential applications in biomaterials, optics and microelectronics [1, 2]. Hashimoto and co-workers [3–5] have performed comprehensive studies on the morphology of blends of block copolymers, starting with blends of lamellae-forming block copolymers. It was shown that a macrophase separation occurs if the ratio of molecular weights is higher than ten, forming macrophase-separated lamellar grains with different long periods. The investigations were also extended to non-lamellar morphologies. Different authors [6] described solubility limits of block copolymer blends.

In spite of recent advances in knowledge of phase behavior of block copolymer blends, only limited investigations have been carried out concerning the influence of morphology on mechanical properties. Only a few studies report on the effect of microphase morphology

*Author to whom all correspondence should be addressed.

on strength and stiffness of block copolymers [7–9] and blends containing block copolymers [10]. While Yamaoka [9] described mechanical properties of thermoplastic SBS, Weidisch *et al*. [7] investigated the influence of phase behavior and loading conditions (strain rate and temperature) on mechanical properties of diblock and triblock copolymers based on polystyrene and poly (*n*-butyl methacrylate). Furthermore, Yamaoka [10] has presented results regarding the influence of processing and composition on toughness (Izod impact strength) of compression- and injection-molded blends of a commercial star-shaped ductile thermoplastic styrene-butadiene-styrene triblock copolymer (SBS) and a brittle methyl methacrylate-styrene copolymer (MS). A macrophase separation between lamellar SBS 'matrix' and MS particles has been found. Here, the SBS/MS blend with 20 wt% MS shows a maximum Izod impact strength. The mechanism of impact toughening of SBS/MS blends is totally different from that of conventional toughened polymer blends (such as ABS or HIPS), where rubber particles are dispersed in the matrix. The effective energy dissipation results from different micromechanical mechanisms: shear yielding in the SBS-Matrix, microcavitation in the polybutadiene lamellae and debonding in the SBS-MS interface [10].

In contrast to fracture mechanics values as resistance against unstable crack propagation, the determination of crack resistance (R) curves as functions of loading parameters versus stable crack growth Δa yields more information about the fracture toughness. Different procedures are available for determination of R curves. Two procedures were developed especially for polymers (ASTM D 6068-96 [11] and Standard Draft ESIS TC4 [12]). However, a standardized R-curve routine that is sufficiently practicable for all polymers, physically motivated and considers both the energy- and deformation-determined fracture toughness due to a multi-parametric description of the crack propagation and fracture behavior is not available up to now. This is mainly attributed to the lack of understanding of kinetics of crack propagation, particularly the processes of crack-tip blunting and initiation of crack propagation. Therefore, the ranges of blunting and small stable crack growth are neglected in a number of R-curve standards (for example in reference [12]). Instead of this, the so-called technical crack initiation values, such as $J_{0.2}$ at a stable crack growth $\Delta a = 0.2$ mm [12], were introduced to quantify the initiation of a stable crack. The empirical procedures mentioned above differ from each other with respect to maximum Δa, J values (limits of validity), the relationship between crack growth and loading parameter, and the determination of the resistance against stable crack initiation and propagation. In addition to these procedures, a physically based R-curve procedure, called the JT_J concept, is suggested by Will [13] (the value JT_J is a measure of the energy dissipation capacity and should be independent of Δa). However, the assumptions used in this model—related to the energy balance (transformation of plastic deformation energy to heat and internal energy) and strain hardening behavior—are only valid for a limited group of materials (mostly metals and ceramics) but typically not for polymers. The functions used to describe crack resistance data are summarized in reference [14].

The application of the crack resistance concept to nanostructured block copolymers was reported in our previous paper [15]. On the other hand, experimental results on crack propagation behavior of other heterogeneous polymer systems under impact loading conditions are well known [16–18]. For conventional heterogeneous polymers, one can conclude that the crack-propagation resistance is strongly morphology-dependent while the crack-initiation resistance reflects the matrix properties [17]. For ductile polymers, two brittle-to-tough transitions (BTT), the conventional BTT and the transition 'tough/high-impact,' corresponding to the resistance against unstable and stable crack propagation, respectively, were observed [19, 20]. It must be emphasized that these morphology-property relationships have been found for conventionally toughened or reinforced polymeric systems, i.e., polymers with matrix-particle structure. However, these correlations have not been studied yet in detail in block copolymer blends, which show nanostructured morphologies. The aim of the present work is to apply fracture mechanics to block copolymer blends to find new concepts for toughening of nanostructured polymer materials.

2. Experimental

2.1. Materials

Binary blends of a star block copolymer (ST2-S74) and a triblock copolymer (LN4-S65), both based on styrene and butadiene, were used in this study. The characteristics of the block copolymers are given in Table I. After mixing the materials in an extruder, the single-edge-notched bend (SENB) and dumbbell specimens were prepared by injection molding (melt temperature 250°C and mold temperature 45°C). The blends contain 5, 10,

TABLE I Characteristics of the blend components and schematic representation of molecular architecture of used materials: (a) ST2 and (b) LN4

Blend component	M_n (g/mol)	M_n/M_w	$\Phi_{styrene}$	Morphology (TEM)
ST2-S74[1]	109,200	1.69	0.74	Lamellar
LN4-S65[2]	116,000	1.20	0.65	PS domains in S/B copolymer matrix

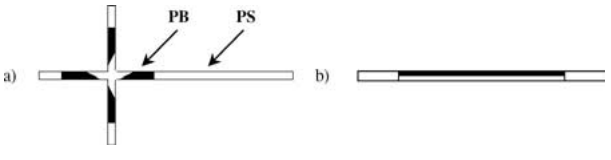

[1]LN4 is a symmetrical triblock copolymer having the block sequence S-S/B-S and weight ratios of 16/68/16. The S/B middle block contains about 50 wt% PS.

[2]ST2 is an asymmetric star block copolymer with about four arms on average with a PS corona and a PB core, which contains a small PS core. ST2 exhibits a tapered transition from the PB blocks to the PS core.

20, 40, 60 and 80 wt% of LN4-S65. Synthesis of these block copolymers is described by Knoll and Nießner [21].

2.2. Tensile test

Uniaxial tensile tests were performed by using the universal electromechanical testing machine INSTRON 4507 at a crosshead speed of 50 mm/min.

The yield stress σ_y was measured from the engineering stress (σ)-strain (ε) diagrams according to ISO 527.

A method to determine the Young's modulus E from the σ-ε curves is the secant procedure according to the standard ISO 527: E is the slope of the secant on the σ-ε curve between $\varepsilon = 0.05\%$ and $\varepsilon = 0.25\%$. But, this method is known not to be very precise for very ductile polymers. Therefore, E moduli were determined by using a tangent procedure, as the maximum slope of the σ-ε curves up to the yield point.

2.3. Determination of fracture mechanics parameter under impact loading

To quantify the toughness behavior of block copolymer blends, an instrumented Charpy impact tester with a maximum work capacity of 4 J was used. Single-edge-notched bend (SENB) specimens with the dimensions $4 \times 10 \times 80$ mm^3 according to standard ISO 179 were used with 2 or 4.5 mm deep sharp edgewise notches. Notches were prepared by using a razor-blade cutter depending on the kind of investigation: the determination of the resistance against unstable crack propagation (2 mm) or stable crack initiation and propagation (4.5 mm), respectively [22]. To minimize the specimen vibrations, the span is set to be equal 40 mm; and the pendulum speed was 1 m/s.

The load-deflection (F-f) diagrams recorded were analyzed with respect to characteristic loading values, deflection and energy (Fig. 1). Dynamic modulus, E_d, dynamic yield stress, σ_{yd}, as well as fracture mechanics parameters as resistance against unstable crack propagation were calculated using the procedure reported in [22]. Here, the investigated fracture behavior of the materials was characterized by means of fracture mechanics parameters of elastic-plastic fracture mechanics such as J integral and crack-tip opening displacement (CTOD). The J values allow the quantification of energy dissipation during the crack propagation process, due to the energetic definition of the J integral. The CTOD values δ_d describe the degree of the deformation close to the crack tip and were calculated using the plastic-hinge model formally extended by replacing the specimen deflection f_{max} at maximum load F_{max} with the 'notch part' f_k of f_{max}:

$$\delta_d = \frac{1}{n}(W-a)\frac{4f_k}{s} = \frac{1}{n}(W-a)\frac{4}{s}\left(f_{max} - \frac{F_{max}s^3}{4BW^3E_d}\right) \tag{1}$$

B, W, a and s are the specimen thickness and width, the notch depth and the span respectively. n is the rotational factor ($n = 4$ in our case).

Due to the predominantly stable crack propagation behavior for blends having LN4 content equal to or higher than 20 wt%, the toughness of these blends could only be characterized by using the crack resistance (R) concept of elastic-plastic fracture mechanics. Using crack resistance (R) curves as a function of loading parameter (J or δ_d) versus the stable crack growth Δa, it was possible to calculate fracture mechanics values describing the resistance against stable crack initiation and propagation. Among different experimental methods to determine R curves [23], the multi-specimen method utilizing a stop-block technique is found to give most exact data [22, 23]. J values were determined using Equation 2

$$J = \frac{\eta_{el}A_{el}}{B(W-a)} + \frac{\eta_{pl}A_{pl}}{B(W-a)}\left(1 - \frac{(0.75\eta_{el}-1)\Delta a}{W-a}\right) \tag{2}$$

where A_{el} and A_{pl}, and η_{el} and η_{pl} are the elastic and plastic part of the deformation energy (Fig. 1), and the corresponding correction functions, respectively [22]. J values calculated by using Equation 2 [22–24] are found to show best agreement with J values calculated by an iterative approximation procedure [23, 24]. For a growing crack it is necessary to correct the J values, i.e., to consider the finite stable growth Δa and also the influence of fluctuations of the stress field ahead the crack tip due to local unloading and dynamic effects

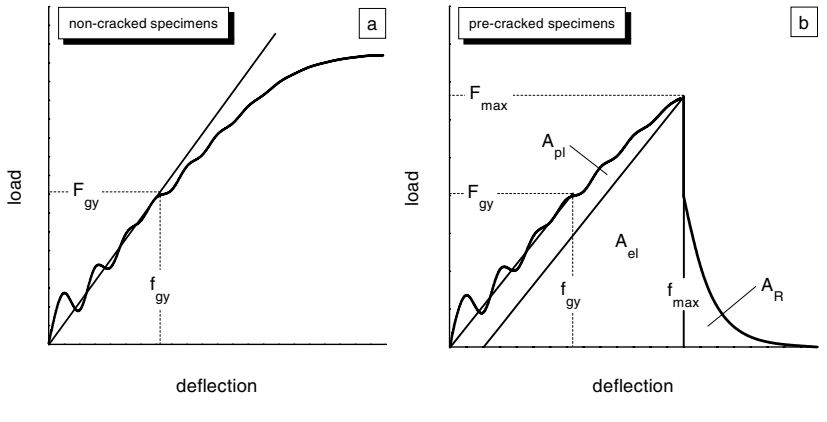

Figure 1 Load-deflection diagrams of non-cracked and pre-cracked specimens. F_{max}, f_{max}—maximum load and deflection at maximum load; F_{gy}, f_{gy}—load and deflection at the transition from linear elastic to elastic-plastic behavior; A_{el}, A_{pl}, A_R—elastic, plastic and crack propagation energy.

(second factor of the second term in Equation 2) because the J integral is defined for a stationary crack only. By using Equation 2, the restrictive requirements for limitation of the size of stable crack growth that is given in the standard draft ESIS TC4 [14] for example [i.e., $\Delta a \leq 0.1(W - a)$] become irrelevant for many polymers—as shown in reference [24]. Nevertheless, the influence of specimen geometry on J and CTOD values still exists. The requirements for geometry independence of fracture mechanics values utilizing R curves may be found in references [22, 25, 26]. Further information about the determination and calculation of R curves under impact loading is summarized in [22].

2.4. SEM investigations of fracture surface morphologies

To correlate microstructure and the fracture behavior to micromechanical processes, analysis of fracture surfaces was carried out by scanning electron microscope (SEM) Jeol JSM-6300. Selected fracture surface zones of SENB specimens broken in the impact test, particularly in the crack-tip blunting region were inspected. The fracture surfaces were sputtered with about 10 nm gold films prior to the SEM analysis and mounted onto special 45° sample holders.

2.5. Dynamic mechanical analysis

Dynamic mechanical analysis (DMA) was carried out by the DTA Torsion Rheometer System (Rheometric Scientific) in torsion and temperature-sweep mode. The measurements were performed with a frequency of 1 Hz, at a temperature range between −120 and 120°C and at a heating rate of 2°C/min. Test specimens of the dimension of 30 mm × 10 mm × 4 mm were prepared from injection molded samples.

3. Results and discussion

3.1. Morphology

Investigations of morphology and phase behavior of block copolymers are usually performed under conditions of thermodynamic equilibrium to understand the influence of molecular architecture on phase morphology of these materials. For technical applications of block copolymers, thermodynamic equilibrium is never achieved, due to the technological constraints like limited processing time (non-equilibrium temperature and deformation regime) and shear stresses. Therefore, analysis of correlation between the non-equilibrium structures (i.e., the influence of processing conditions) and mechanical properties must be considered in detail. A comparison of the equilibrium morphology of sample ST2 with an injection molded morphology clearly demonstrates a substantial influence of processing (especially due to the high shear rate during injection molding) on the morphology of the block copolymer (Fig. 2a). High shear stresses lead to preferential orientation and pronounced long-range order of the lamellae along the injection direction. In contrast to amorphous polymers such as homopolymers or matrix materials in macrophase-separated polymer blends, the chains are oriented perpendicular to the lamellae interfaces for entropic reasons (and normal to the flow direction). In contrast, the equilibrium morphology of ST2 films prepared from solution (toluene) consists of lamellae comprising grains with different orientations (isotropic macrostructure) [39]. Equilibrium morphologies of samples ST2 and LN4 comprise alternating polybutadiene (PB) and polystyrene (PS) lamellae with additional PS domains inside the PB lamellae and randomly distributed PS cylinders in a styrene-butadiene copolymer matrix [40], respectively.

While the influence of processing on morphology of pure LN4 is less pronounced than that of pure ST2 (Fig. 2d), the macrophase separation in the injection molded blends of ST2 and LN4 is suppressed by the shear stresses in the melt during injection molding (Fig. 2c and b). Basically, two types of morphologies are found in the injection-molded blends due to partial miscibility (see results of DMA, Fig. 3) of ST2 and LN4. Characteristics of the lamellar morphology found in pure ST2 also predominate at lower LN4 content (0–20 wt% LN4). The microphase-separated structures at higher LN4 content (40–80 wt% LN4) are similar to pure LN4. A structural reorganization ('disorder') appears with increasing LN4 content, which strongly influences the achieved level of toughness and underlying crack propagation mechanisms. For the following discussion results from injection-molded samples will be used.

Partial miscibility of ST2/LN4 blends is proved by shifts in glass transition temperatures (T_g s) depending on composition (Fig. 3). The higher the LN4 content, the higher the T_g of the rubber phase and the lower the storage modulus (G') due to increasing mixing of PS blocks and butadiene-rich blocks within the rubber domains. Increasing interfacial volume fraction can be observed due to increasing plateau values of the loss factor ($\tan \delta$) for temperatures above the T_g of the rubber phase. This leads to weaker segregation of the PB-rich and PS-rich domains resulting in a mixed microphase separated morphology.

In contrast to conventional polymer blends, where a soft phase (e.g., rubber) is dispersed in the brittle matrix, a phase inversion is not observed in the blends of ST2 and LN4. This results from the absence of macrophase separation of corresponding block copolymer microdomains due to the high shear stress of injection molding, and from partial miscibility of the similar block domains of the constituent block copolymers.

In contrast to microphase-separated morphology of the injection-molded samples, films prepared from solution (toluene) show a macrophase separation with dispersed LN4 domains in the ST2 matrix, which represents the equilibrium structure of this blend [15]. Our investigations clearly show that the phase separation occurs on the nanometer scale and the materials do not show turbidity, thus the materials can still be used for applications as transparent components.

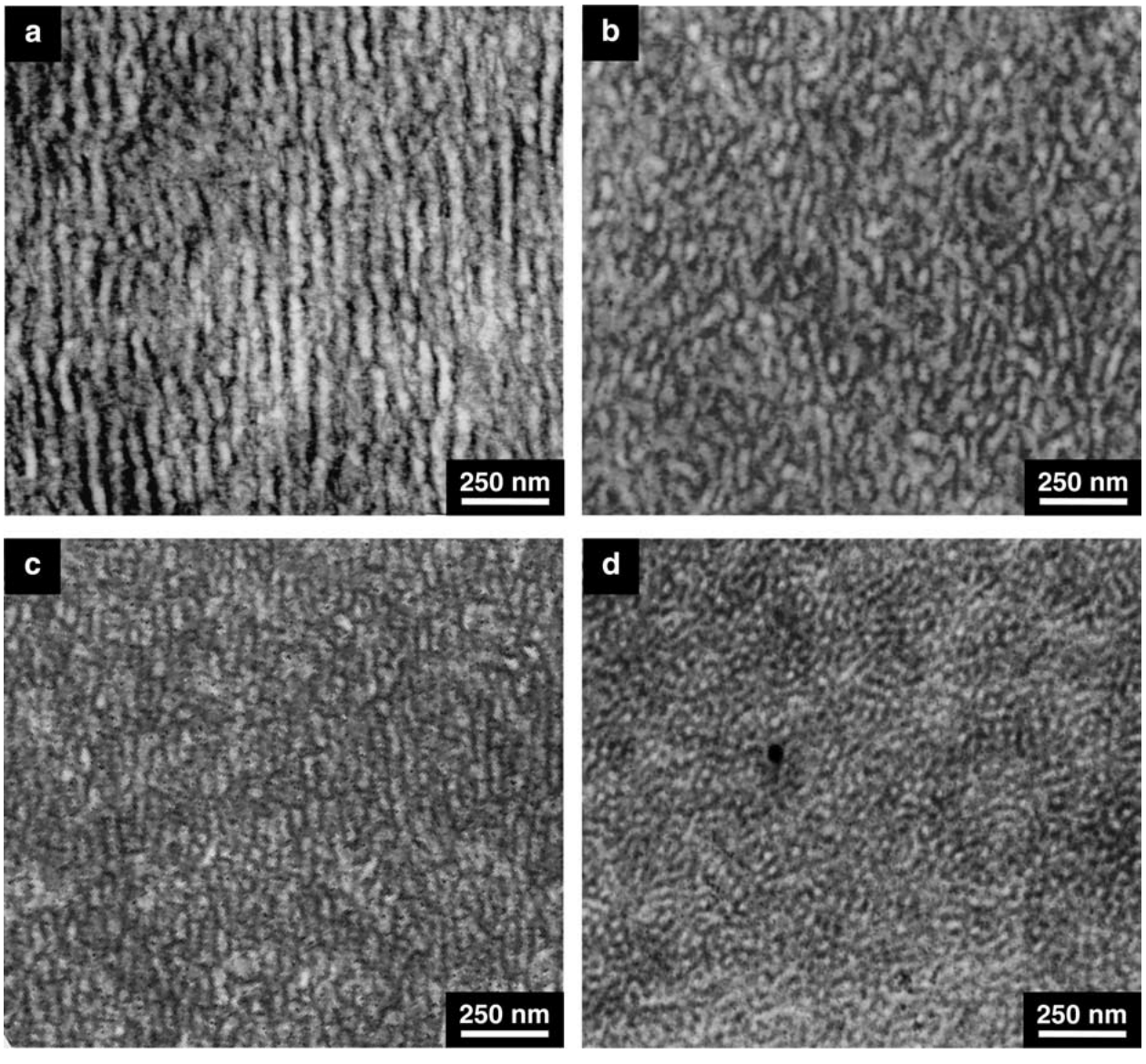

Figure 2 TEM micrographs of injection-molded ST2/LN4 block copolymer blends: (a) ST2, (b) 20 wt% LN4, (c) 40 wt% LN4, and (d) LN4 (stained with OsO_4); dark areas: PB domains and light areas: PS domains (reproduced from [15]).

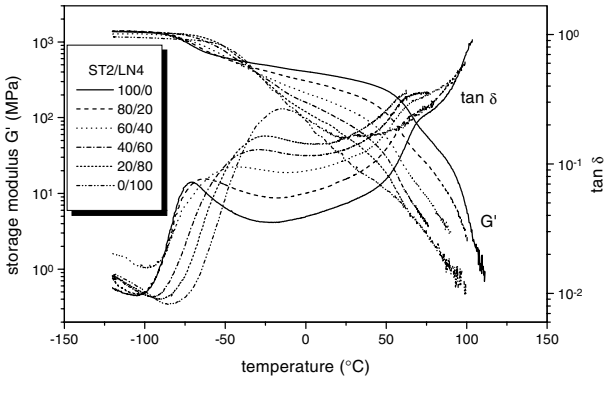

Figure 3 Mechanical loss factor tan δ and storage modulus G' for ST2/LN4 blends.

3.2. Mechanical behavior

Morphology and tensile properties of a very similar system were discussed by Knoll and Nießner [21]. This system did not show any loss of transparency over the whole composition range and showed a linear dependence of tensile strength and strain at break (uniaxial tensile test at 50 mm/min). Fig. 4 shows clearly the changes in mechanical behavior expressed by stress (σ)-strain (ε) diagrams of the ST2/LN4 blends. With increasing LN4 content, the σ-ε diagrams change from

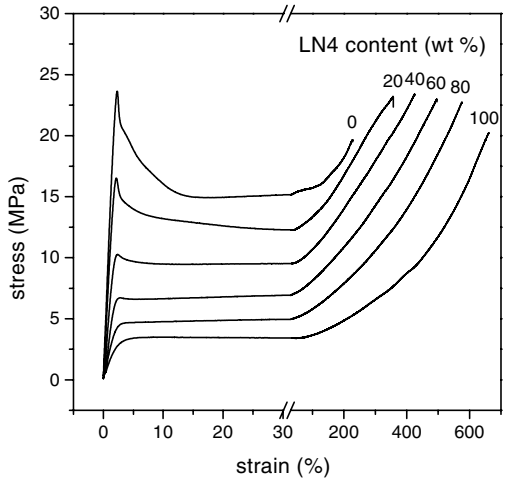

Figure 4 Stress (σ)-strain (ε) curves for ST2/LN4 blends.

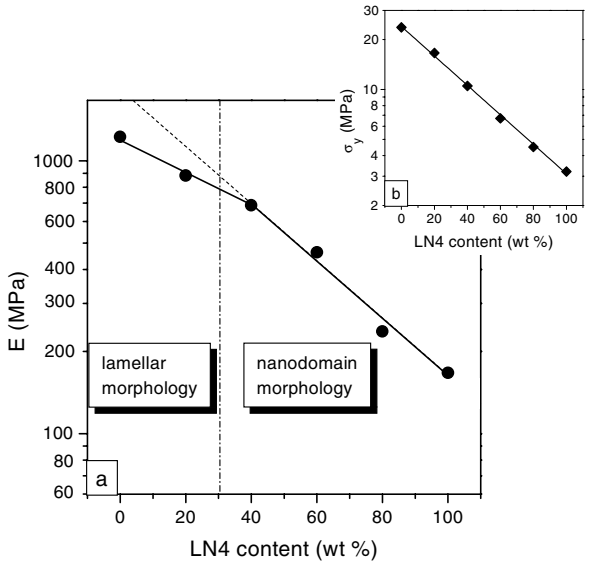

Figure 5 Elastic modulus (a) and yield stress (b), E and σ_y, for ST2/LN4 blends, the broken line marks an exponential shape of E.

a shape that is typical for a conventional thermoplastic polymer to one that is typical for a TPE. The absence of macrophase separation can also be demonstrated by the dependences of the yield stress σ_y and the dynamic yield stress (σ_{yd}) on composition, which exponentially decrease with increasing LN4 content in the blends (Figs 5b and 6b).

In contrast to conventionally toughened polymers, the percolation of the rubber phase in ST2/LN4 blends already exists in the matrix material (pure ST2) due to the PS and PB lamellae orientated in the loading direction. This results in a non-exponential shape of modulus versus LN4 concentration curve up to 20 wt% LN4. With increasing LN4 content, the percolation breaks up leading to a microdomain structure in the range of nanometers (nanodomains), and E and E_d show an exponential dependence on the composition (Figs 5a and 6a).

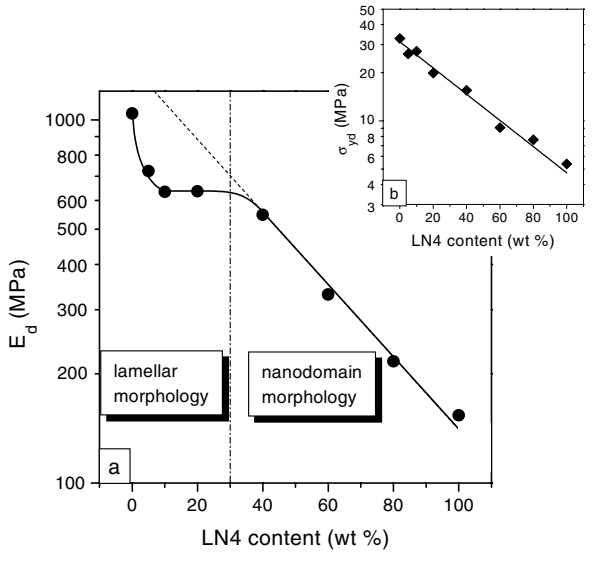

Figure 6 Dynamic elastic modulus (a) and dynamic yield stress (b), E_d and σ_{yd}, for ST2/LN4 blends, the broken line marks an exponential shape of E_d.

3.3. Crack resistance curves

For sharply notched specimens of the blends, only small plastic deformation of the materials was observed up to 20 wt% LN4. Since the maximum stable crack growth in this composition range was very small ($\Delta a \leq 70\,\mu$m, small scale yielding), crack arrest is generally impossible (unstable fracture). Hence, the experimental determination of crack resistance curves (R curves), i.e., the relation between fracture mechanics parameters (J integral J_d as well as crack tip opening displacement, CTOD δ_d) and stable crack growth Δa was only possible at LN4 weight fractions equal to or larger than 20%. The quantitative description of stable crack propagation behavior is based on fracture mechanics parameters as resistance against stable crack initiation and stable crack propagation. The technical crack initiation values determined at an arbitrary value of Δa (here, $J_{0.05}$ and $\delta_{0.05}$ are determined at $\Delta a = 0.05$ mm instead of 0.2 or 0.1 mm usually found in standards and literature) are taken into account in order to characterize the stable crack initiation. Furthermore, because crack initiation is followed by crack propagation and occurs at larger Δa values, $\Delta a = 0.1$ mm is used to determine the resistance against stable crack propagation. Physical crack initiation values (J_i and δ_i) can also be determined based on the consideration of the kinetics of crack propagation processes, i.e., analysis of different phases of crack growth (crack-tip blunting, stable crack initiation and propagation, unstable crack propagation) as a function of time. One possibility of determining these parameters is demonstrated in Fig. 7 (J_i is determined at the onset of Δa versus time). Additionally, conclusions about the magnitude of physical crack initiation values can be derived from the quantitative analysis of the crack-tip blunting zone (stretch zone) on fracture surfaces. Because the latter procedure is relatively time consuming, technical crack propagation values are usually determined. The slope of the R curves at $\Delta a = 0.1$ mm (i.e., $dJ/d(\Delta a)|_{0.1}$ and $d\delta/d(\Delta a)|_{0.1}$) and resulting tearing modulus ($T_J = dJ/d(\Delta a)|_{0.1} \times E_d/\sigma_{yd}^2$ and $T_\delta = d\delta/d(\Delta a)|_{0.1} \times E_d/\sigma_{yd}$) are determined to characterize the resistance against stable crack propagation. As shown in Fig. 8a and b, R curves with

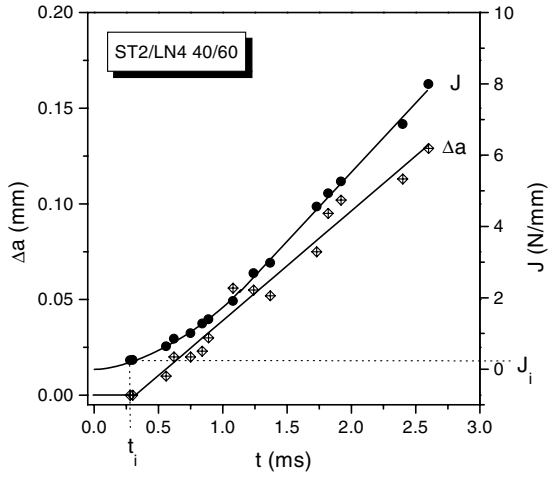

Figure 7 Determination of physical initiation values J_i from $\Delta a(t)$ and $J(t)$ plots.

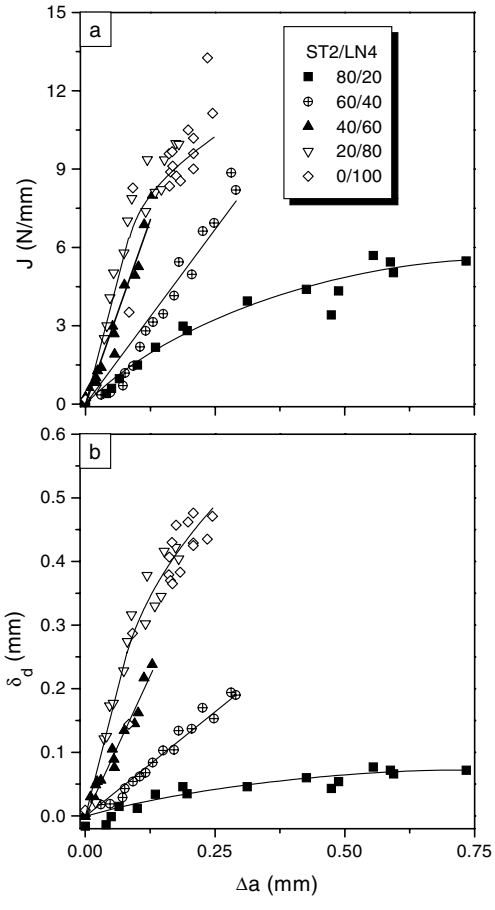

Figure 8 Crack resistance curves (R curves) for ST2/LN4 blends with (a) J and (b) δ_d as loading parameter.

J or δ as loading parameter exhibit similar dependencies. As reported in [15], slopes of the R curves at $\Delta a = 0.1$ mm and tearing modulus increase with LN4 concentration up to 80 wt% and remain constant at higher LN4 contents. In the present case, the increasing ductility measured for unnotched samples as a function of LN4 content (compare Fig. 4) is also reflected in the increasing resistance against stable crack propagation. It should be, however, mentioned that this correlation does not have a general validity as shown by our recent results [27], where the opposite has been found due to the strongly material-dependent notch sensitivity.

3.4. Kinetics of crack propagation

The kinetics of crack growth, especially also the demarcation of each stage of crack growth, can be described by the velocity of crack propagation da/dt. Additionally, it can be described by the derivation of fracture mechanics parameters like CTOD rate, dδ/dt (Fig. 9). The maximum velocity of crack growth attained during stable crack propagation decreases with increasing LN4 content: 0.6 m/s for the blend with 20 wt% LN4, 0.12 m/s for the blend with 40 wt% LN4 and 0.05 m/s for the blends having $\geq$60 wt% LN4. These values correlate well with increasing resistance against stable crack growth as shown in Fig. 10 (discussed later).

Fig. 9 shows that different stages of crack propagation are represented by different slopes of dδ/dt values. Stage I correlates with the region of crack-tip blunting,

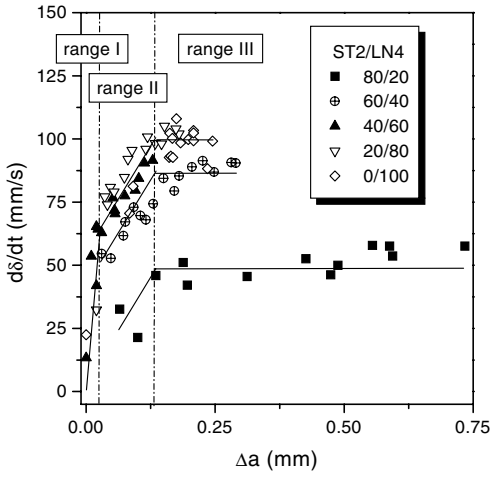

Figure 9 Crack-tip opening displacement rate dδ/dt in dependence on the stable crack growth Δa for ST2/LN4 blends.

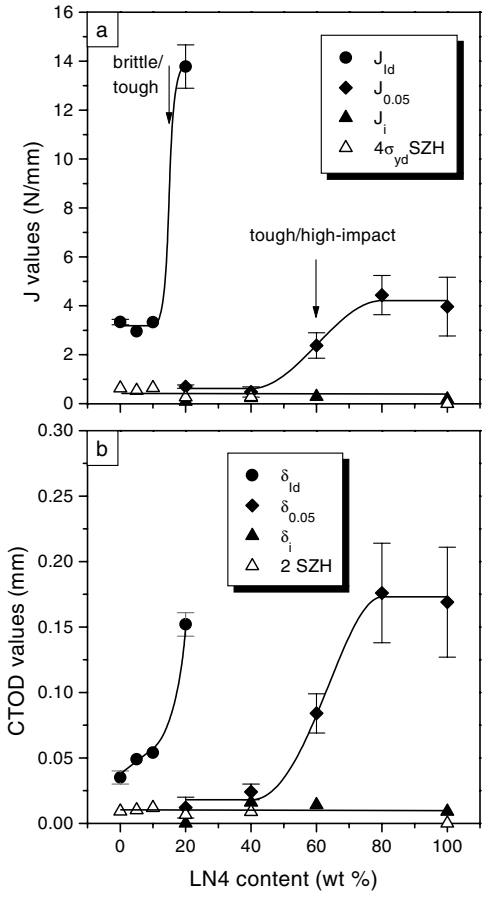

Figure 10 Technical initiation values, $J_{0.05}$ and $\delta_{0.05}$, and physical initiation values, J_i and δ_i, as resistance against stable crack initiation and values, J_{Id} and δ_{Id}, as resistance against unstable crack propagation for ST2/LN4 blends as a function of weight fraction of LN4: (a) J_{Id}, $J_{0.05}$, J_i and $4\sigma_{yd} \times$ SZH, (b) δ_{Id}, $\delta_{0.05}$, δ_i and $2 \times$ SZH.

where the initial razor-sharp crack blunts resulting in a rapid increase in the dδ/dt values. In the Stage II, the crack moves in a quite stable but non-steady way, i.e., the dδ/dt values still increase with Δa. In Stage III, the non-steady stable crack finally reaches a (quasi-)steady state, and the value of dδ/dt remains approximately constant. The significance of constant dδ/dt values is nearly equivalent to that of constant crack-tip opening angles (CTOA). The maximum value of dδ/dt attained

increases with LN4 content in the blends: 0.05, 0.09 and 0.10 m/s for 20 and 40 wt%, and 60–100 wt% LN4 respectively.

The opposite behavior of $d\delta/dt$ and da/dt as a function of LN4 fraction is related to the different physical meaning of these two parameters. da/dt indicates the compliance of the whole mechanical system and, consequently, it is dependent on the brittleness of cracked specimens (form and size of specimens, materials), the internal stiffness of the testing devise and the type of loading (strain-rate or stress-rate controlled loading, bending or tensile loading etc.). But in case of constant external conditions (well-defined specimens and loading conditions including constant temperature and test speed)—as in the present study—the compliance is only influenced by the material used. Therefore, the velocity of crack propagation should increase with decreasing toughness (J), which can be experimentally observed (Fig. 10). In contrast to da/dt, $d\delta/dt$ is also a function of the type of deformation and the polymer phase predominantly deformed during the deformation process because the CTOD is a measure of the deformation of the material close to the crack tip. Thus, the threshold of CTOD rate should give an insight into the micromechanics and the activation mechanisms of the fracture process [28].

3.5. Analysis of fracture behavior

Fig. 10 shows fracture mechanics parameters as a function of LN4 content. The indices '0.05' and 'i' represent the technical and physical crack initiation values, respectively, as resistance against stable crack propagation determined at $\Delta a = 0.05$ mm and from Fig. 7. The values indexed as 'Id' represent the resistance against unstable crack propagation. The physical crack initiation values J_i are not influenced by the morphology of the materials, which is in accordance with previous results on heterophase polymeric materials [17]. This means, that the crack initiation values are quite insensitive to the change of morphology, which has been shown for both heterophase polymers [29] and metals [30]. It is, however, not true in the case of crack propagation values. Thus, usually only J_i and J_{Id} can be considered as the relevant toughness parameters related to well-defined fracture processes. These values (i.e., J_i and J_{Id}) can be clearly correlated to the processes of stable crack initiation and unstable crack propagation, respectively. Notwithstanding, the technical crack initiation values $J_{0.05}$ show a pronounced dependence on the LN4 content and do not correspond to the end of the crack-tip blunting process due to the arbitrary assumption of Δa. Nevertheless, owing its relatively straightforward determination, $J_{0.05}$ is also very useful as a material parameter.

3.5.1. Brittle-to-tough transitions

The application field of heterogeneous polymeric materials is often limited by the brittle-to-tough transition (BTT) temperature and the critical modifier concentration. Generally, this transition is determined as an average value of high and low plateau values of toughness, where, unfortunately, the conventional notched impact strength is mostly used. However, this approach becomes especially difficult when a correlation between structure, toughness-determined deformation mechanisms and BTT should be derived. The conventional notched impact strength is an integral magnitude, which allows neither the independent consideration of different energy components (like elastic and plastic deformation energy, crack-propagation energy etc.) involved during the process of crack growth, nor the separate evaluation of resistance against stable crack initiation, stable crack propagation and unstable crack propagation [31]. It should be further stressed that this approach could produce misleading results by attributing equivalent impact strength (i.e., equivalent total energy) to materials showing different force-deflection curves [28].

According to the present investigation, two different BTTs were also observed in heterophase PP systems [19] and ABS [20]: the conventional 'brittle/tough' transition (BTT 1) and the second one BTT 2. In contrast to the BTT 1 as a measure for the safety against unstable crack propagation, the BTT 2 can be described as a measure for the safety against stable crack propagation. While a pronounced BTT 1 can be observed at 20 wt% of LN4, a quite wide BTT 2 is located at 60 wt% of LN4. As demonstrated recently [19, 20], BTT 1 occurs if the crack growth mechanism changes from unstable towards stable one. Here, this behavior is combined with a change in the predominant microdeformation process in the plastic zone ahead the crack tip (change from thin-layer yielding and coalescence of holes to shear flow, see below). Furthermore, the BTT 2 should also be correlated to a change in microdeformation mechanism, probably the transition from shear flow to rubber-like tearing. For conventionally toughened polymers [19], differences in deformation mechanisms associated with BTT 1 and BTT 2 can be explained by Wu's percolation concept [32] and Margolina's concept [33], respectively. Wu [32] has been introduced a critical interparticle distance, ID_c, which is correlated with a BTT. He assumed that ID_c is characteristic for a given matrix and can be explained by stress-field overlap (percolation) of neighboring particles. However, this model is questioned because the overlap of local stress concentrations of neighboring particles does not occur until the ratio between the interparticle distance and the particle size is less than or equal to 0.5 [34] and is usually a constant for a given material. Margolina [33] has further shown that a BTT associated with an ID_c can be observed if the yielding propagates through thin matrix ligament, where a plane strain to plane stress transition takes place. Temperature effects and loading conditions are incorporated in this model and concludes that the ID_c is not a constant for a given material. Especially, the critical interparticle distance shows nearly a linear dependence on temperature. Such a simple classification is, however, not expected in the investigated systems due to the absence of particle-matrix structure typical of polymer blends, where the particle diameter ranges

from few hundred nanometers to a few micrometers. In contrast, the structural heterogeneity in the systems investigated in this study lies on nanometer scale, which is associated with the BTT 1 as discussed in detail below.

3.5.2. Mechanisms of microdeformation and crack propagation

In-situ investigation using TEM is one possibility for analyzing the microdeformation and crack propagation mechanisms, another is the study of fracture surfaces exemplary by SEM. The last is used here, which allows the crack propagation phenomenon to be analyzed (Figs 11 and 12). ST2 undergoes brittle failure right after the crack-tip blunting, through unstable crack propagation (Figs 11a and 12a). A small but noticeable amount of stable crack growth can be observed ahead of unstable crack growth for blends with 5 (Figs 11b and 12b) and 10 wt% LN4. The stable crack growth is shown in the SEM micrographs by coalescence of microvoids as indicated by dimple-like patterns. Such a crack propagation mechanism is typical for semicrystalline polymers like HDPE [35], where the lamellae structures are on the nanometer scale as well. As shown by SEM micrographs presented in Fig. 11, the transition BTT 1 is not only associated with a strong increase in stability of the crack propagation process but also with a fundamental change in the crack propagation mechanisms. In a composition range of 10–20 wt% LN4, as a consequence of increasingly disordered morphology, a change in stable crack propagation mechanism from coalescence of microvoids to shear flow occurs. The individual crack growth planes (fracture parabolae) are separated by clearly visible shear lips (Fig. 11c). Crack growth via shear flow is typical for many tough or semi-brittle amorphous polymers like polycarbonate [31]. Here, the crack becomes again sharp after blunting and moves through the entire material by translation of the whole crack front [36]. This leads to a stretch zone at the end of the entire fracture mirror length (Fig. 12c) in contrast to the stretch zone formed at the end of razor notch in the blends containing 5 (Fig. 12b) and 10 wt% of LN4. The geometry of the stretch zone can be taken into account as a measure for plastic deformation during crack-tip blunting, which is indicated as "stretch-zone width" (SZW) along the crack propagation direction and as "stretch-zone height" (SZH) perpendicular to the crack growth direction. The decrease of SZW in the blends with increasing LN4 content (Fig. 13a) may be attributed to the transition from a conventional thermoplastic (ST2) to a thermoplastic elastomer (LN4), i.e., a transition from viscoelastic to entropy-elastic deformation behavior.

For materials having pronounced plastic deformation, the dimensions of the crack-tip blunting zone is

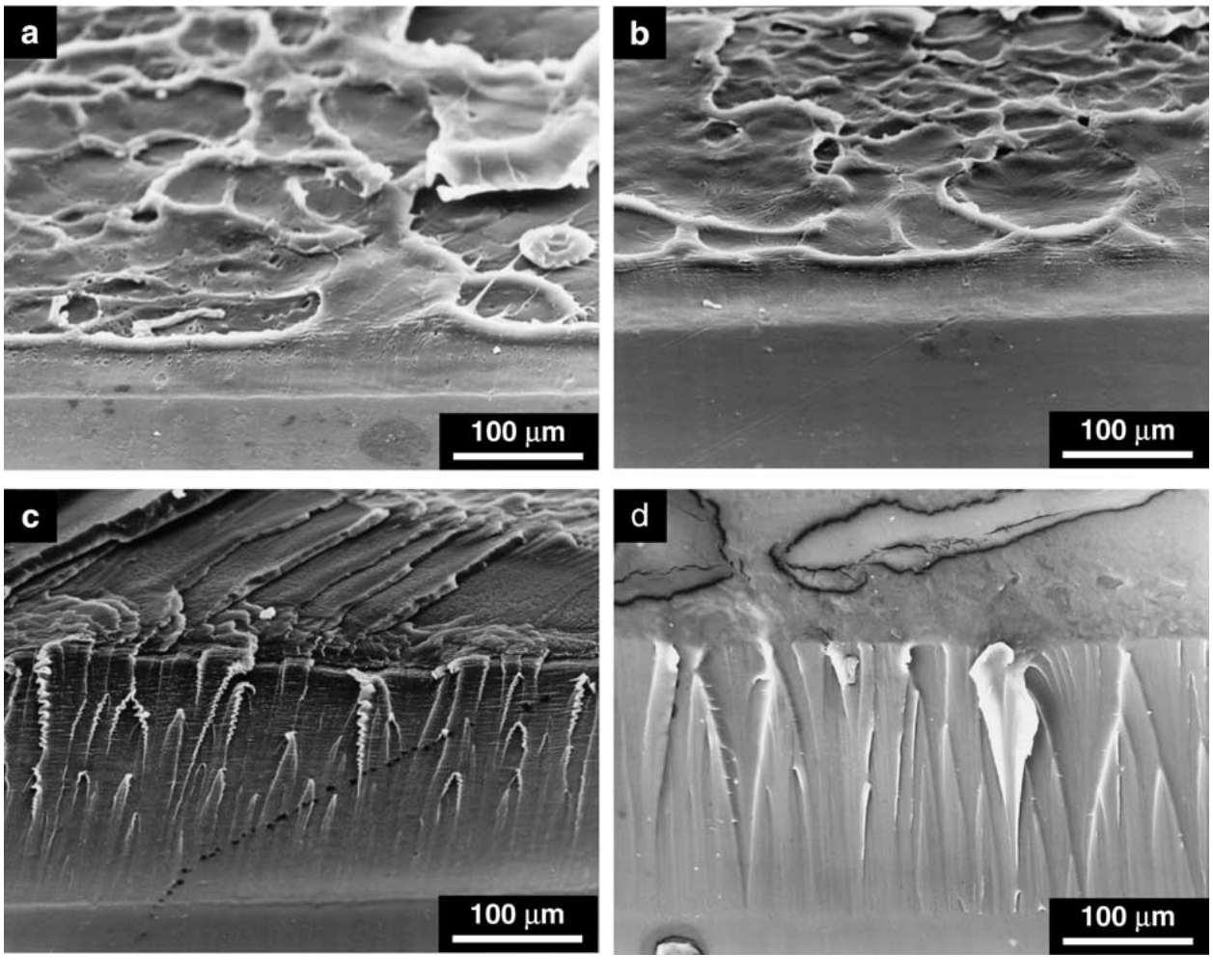

Figure 11 SEM micrographs of the fracture surface for ST2 (a), ST2/LN4 blends with 5 wt% LN4 (b) and 40 wt% LN4 (c), and LN4 (d).

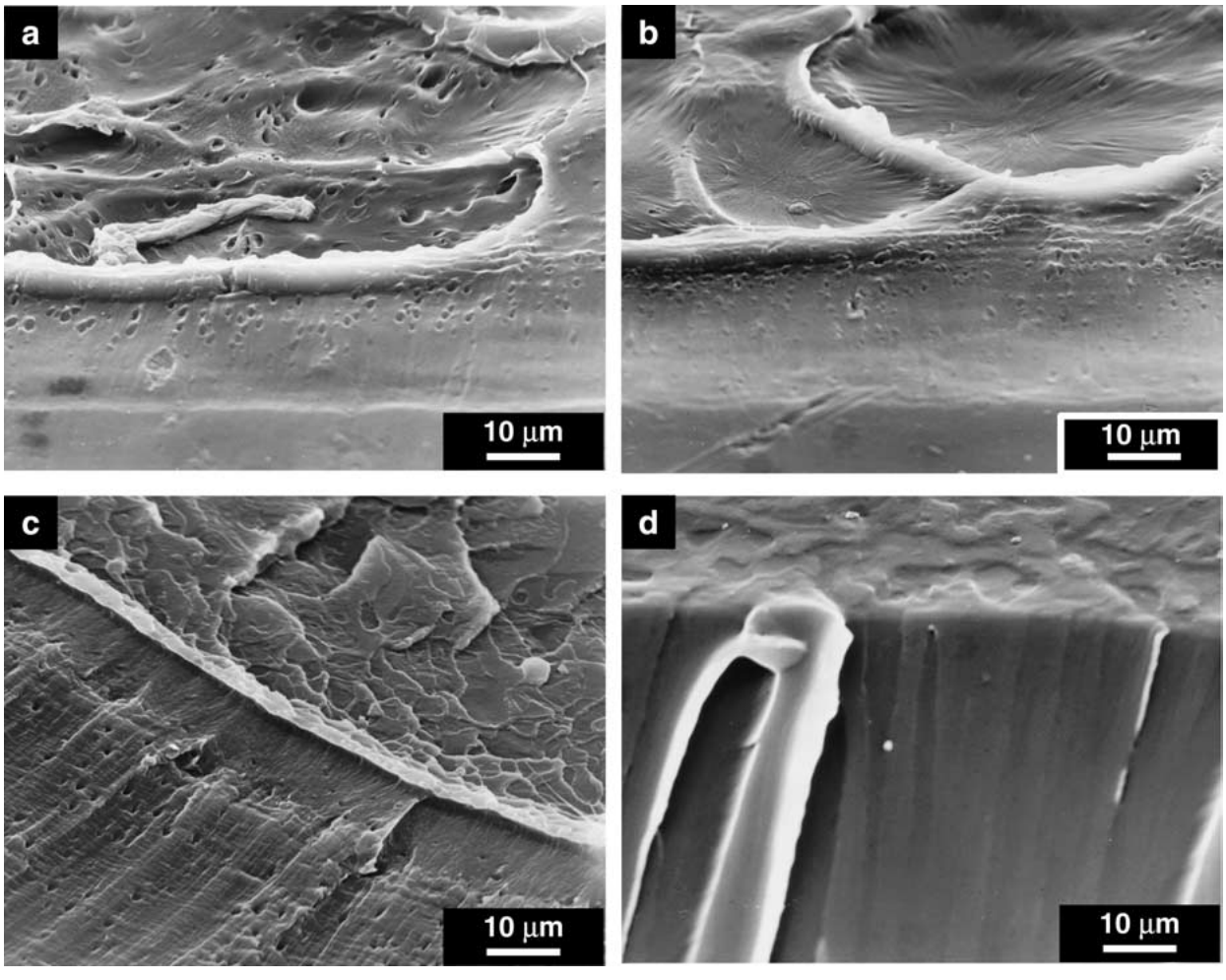

Figure 12 SEM micrographs of the crack-tip blunting region (stretch zone) for ST2 (a), ST2/LN4 blends with 5 wt% LN4 (b) and 20 wt% LN4 (c), and LN4 (d).

only little influenced by elastic strain recovery, so that the SZH is useful to estimate physical crack initiation values δ_i, where $\delta_i \approx 2 \times$ SZH. Except for pure LN4 (predominant entropy-elastic deformation behavior), the δ_i values ($\delta_i \approx 10\ \mu$m) determined from Fig. 7 are in good agreement with the δ_i value ($\delta_i = 9.3 \pm 1.9\ \mu$m) measured from stretch zones (Fig. 10b). The J_i values (Fig. 10a) calculated by Equation 3.

$$J_i = m \times \sigma_{yd} \times \delta_i = 4\sigma_{yd} \times \text{SZH} \qquad (3)$$

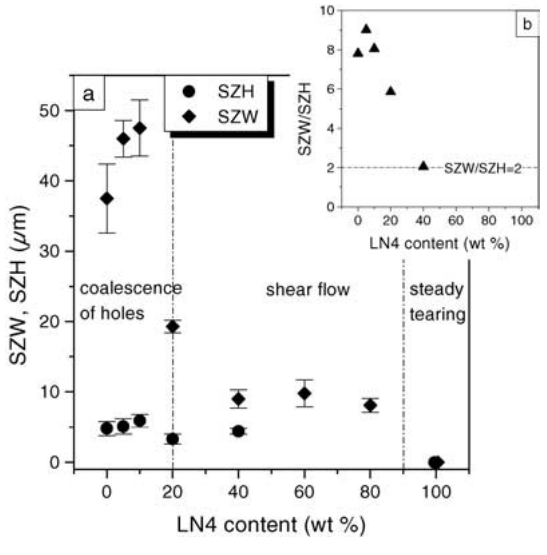

Figure 13 Stretch-zone width (SZW), stretch-zone height (SZH) (a) and ratio between SZW/SZH (b) as a function of weight fraction of LN4.

(with $m = 2$ and $\delta_i \approx 2\times$ SZH, m—constraint factor depends on the state of stress)—using the SZH values and the general relationship between J integral and CTOD—are in agreement with J_i values determined by Fig. 7 ($J_i \approx 0.2$ N/mm, $\geq$20 wt% LN4). The ratio SZW/SZH (Fig. 13b), determining the shape of the stretch zone, is a measure for the type of deformation process during crack-tip blunting [24]. The stretch zone is wedge-shaped if the crack-tip blunting process results from the coalescence of holes, i.e., SZW/SZH $\gg$ 2. If shear flow occurs, the profile of the stretch zone is more circular with SZW/SZH $\lessapprox$ 2 (empirical values for polymers [37]). The ratio SZW/SZH decreases significantly with increasing LN4 content due to increasing amount of shear yielding (Fig. 13) also supporting the conclusion of a BTT 1 at 20 wt% LN4. For materials containing $\leq$10 wt% LN4, high SZW/SZH values of 8.3 $\pm$ 0.6 are measured. In contrast, for blends with 20 and 40 wt% LN4, SZW/SZH values of 5.8 and 2.0

are found, respectively. The latter value is in agreement with a shear flow process (compare with Fig. 11c). For pure LN4, a stretch zone is not observed due to the rubber-type steady tearing of this material (Figs 11d and 12d).

3.5.3. Rheological model

In contrast to conventional polymer blends, where the toughness modification is achieved through the dispersion of a soft phase in a hard matrix (macrophase separation), the investigated binary block copolymer blends represent nanometer-structured materials. A new mechanism of toughness modification (in which the transition from a lamellar structure with a pronounced long-range order to a locally ordered structure plays the central role) results in specific properties-toughness correlations, which fundamentally differ from the toughness modification of conventional polymer blends. However, as for conventional particle-matrix structured materials [38], a heterogenization of structure is necessary for increasing the toughness under impact as well.

For blends containing 0–10 wt% LN4 (lamellar morphology), the PS and PB-rich lamellae are perpendicularly oriented to the crack propagation direction but the polymer chains are oriented normal to lamellae. This lamellar morphology under load corresponds to a model of serial-combined mechanical resistors (springs with non-linear stress-strain characteristic) This means that, at increasing strains, stresses in PS lamellae already reach the local tensile strength of PS whereas only small stresses, much lower than the local tensile strength of PB exist simultaneously in the PB-rich lamellae. This mechanism is intensified by the plane strain state due to the use of compact specimens with sufficiently large thickness under bending conditions (SENB), by high loading rates (1 m/s), and if the lamellae are chemically coupled by polymer chains. As a result, the thickness of lamellae decreases and their respective length increases during deformation (thin-layer yielding was found experimentally [39]). Thus, hydrostatic pressure is generated in PB-rich domains ('conventional' Poisson's ratio: $\nu \approx 0.5$) and hydrostatic tensile stress acts in PS (conventionally, nearly volume constancy, i.e., $\nu \approx 0.5\sqrt{0.5} = 0.35$), respectively. The latter may lead, at a critical value of loading, to cavitation in the PS followed by coalescence of holes. These holes act as flaws, leading to premature crack propagation. Thus, the energy dissipation is small. The time dependence of the thin-layer-yielding process and microcavitation in PS also plays a role.

For blends with 40–100 wt% LN4 under loading the situation is more complex and cannot be approximated by a simple combination of mechanical resistors, due to the non-lamellar nanodomains structure of PS and rubber phase. Local strains in the rubber phase are much higher than in the PS phase, theoretically leading to microcavitation in the rubber phase (but the large surface energy due to the small curvature of the rubber domains may prevent this). This behavior leads to increasing energy dissipation and crack propagation stability by shear flow or steady tearing.

The blend with 20 wt% LN4 takes an intermediate position with regard to the morphology (order-disorder transition, see chapter '3.1. Morphology') and the deformation processes (transition from hole formation to shear flow, see above), so that the BTT 1 is observed at this composition.

The morphology-property correlations concluded above could be also discussed on the basis of the crack propagation kinetics, where the process of stable crack propagation can be thermodynamically described as a kinetic phenomenon on the basis of a two-potential model. Based on discussion in reference [28], the large $d\delta/dt$ values of pure LN4 and blends containing large amounts of LN4 combined with smaller activation enthalpy (determined from the yield stress as a function of reciprocal temperature) for deformation of PB-rich materials (80 kJ/mol), compared to that of PS-rich materials (180 kJ/mol), leads to the conclusion that mainly the PB-rich domains are locally deformed. With decreasing LN4 content, the enhanced local deformation of PS is reflected by decreasing $d\delta/dt$ values (serial-combined mechanical resistances).

4. Conclusions

This study represents an investigation of the crack resistance behavior of binary block copolymer blends. In contrast to current trends to develop novel polymeric materials based on binary polymer blends such as PP/EPDM, ethylene-propylene copolymers, and other high-impact PP materials, the binary SB block copolymer blends, consisting of a thermoplastic block copolymer (ST2) and a TPE (LN4), investigated in this study combine high-impact behavior with excellent transparency, and allow the stiffness-toughness ratio to be adjusted over a wide range. Two transitions are observed with increasing LN4 content, the conventional 'brittle/tough' transition, and the 'tough/high-impact' transition. While the former is caused by the transition from unstable to stable crack propagation, the 'tough/high-impact' transition should be caused only by a transition in deformation mechanism. In contrast to sample ST2, materials with about 60 wt% LN4 reveal a sufficiently high toughness for application under impact loading and still maintain their high level of transparency. The correlation between morphology, fracture toughness and deformation mechanisms as a function of LN4 content can be described by a transition in the material behavior that is similar to that of lamellae-structured semi-crystalline polymers, amorphous polymers, and elastomers (Fig. 14). It should be mentioned that the morphology-toughness correlation observed in the block copolymer blends is fundamentally different from that found in conventional impact-modified or reinforced polymeric systems with matrix-particle morphology due to their nanometer-structured morphologies. Our investigations have demonstrated that utilizing blends of block copolymers can lead to new materials concepts for toughened and transparent nanostructured polymer materials.

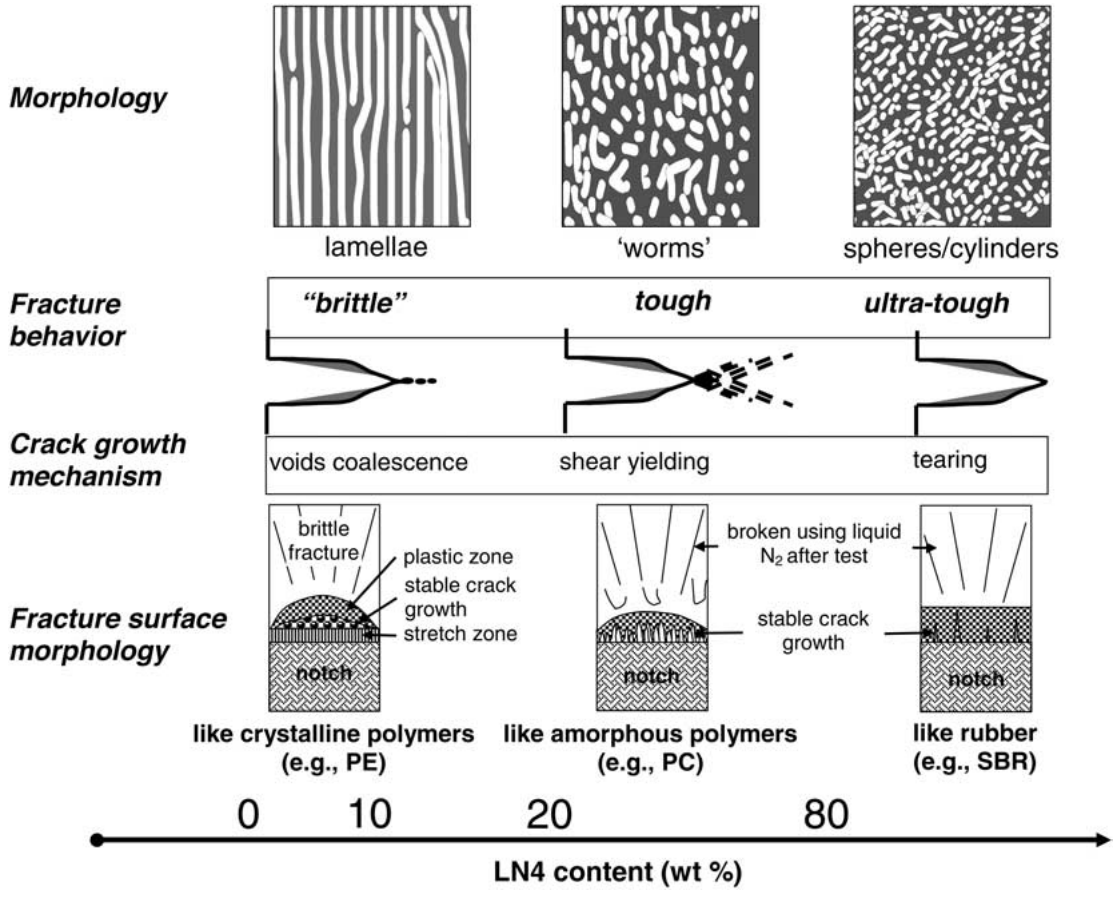

Figure 14 Scheme of the correlation between morphology, fracture toughness and deformation mechanisms in ST2/LN4 blends.

Acknowledgements

The authors would like to thank BASF for fruitful collaboration and synthesis of the materials, and for authorization of publication. R. W. acknowledges Heisenberg Fellowship from German Research Foundation (DFG). R. A. thanks the Max-Buchner Research Foundation and the Ministry for Culture of Saxony-Anhalt (project: 'New functional materials based on weakly segregated block copolymers') for financial support. The authors thank Mrs. S. Goerlitz for TEM measurements.

References

1. D. A. TIRELL, *Nature* **390** (1997) 336.
2. Z. R. CHEN and J. KORNFIELD, *Polymer* **39** (1998) 4679.
3. T. HASHIMOTO, S. KOIZUMI and H. HASEGAWA, *Macromolecules* **27** (1994) 1562.
4. T. HASHIMOTO, K. YAMASAKI and S. KOIZUMI, *ibid.* **26** (1993) 2895.
5. S. KOIZUMI, H. HASEGAWA and T. HASHIMOTO, *ibid.* **27** (1994) 4371.
6. I. W. HAMLEY, "The Physics of Block Copolymers" (University Press, Oxford, 1998).
7. R. WEIDISCH and G. H. MICHLER, in "Block Copolymers," edited by F. Balta Calleja and Z. Roslaniec (Marcel Dekker Inc., New York, 2000) p. 215.
8. "Thermoplastic Elastomers," edited by N.R. Legge, G. Helden, H. E. Schroeder and R. P. Quirk (Carl Hanser, Munich Vienna, 1996).
9. I. YAMAOKA and M. KIMURA, *Polymer* **34** (1993) 4399.
10. I. YAMAOKA, *ibid* **39** (1998) 1765.
11. ASTM D 6068, "Standard Test Method for Determining J-R Curves of Plastics" (ASTM, Philadelphia, 1996).
12. Standard Draft ESIS TC4, "A Testing Protocol for Conducting J-Crack Growth Resistance Curve Tests on Plastics" (ESIS, Sheffield, 1995).
13. P. WILL, *J. Mater. Sci.* **29** (1994) 2335.
14. W. BROCKS, G. KÜNECKE and T. STEIGER, BAM Research Report No. 1.01 91/3 (BAM, Berlin, 1991).
15. R. ADHIKARI, R. LACH, G. H. MICHLER, R. WEIDISCH, W. GRELLMANN and K. KNOLL, *Polymer* **43** (2002) 1943.
16. "Fracture Mechanics Testing Methods for Polymers, Adhesives and Composites" (ESIS Publication 28), edited by D. R. Moore, A. Pavan and J.G. Williams (Elsevier Science, Amsterdam, 2001).
17. "Deformation and Fracture Behaviour of Polymers," edited by W. Grellmann and S. Seidler (Springer, Berlin Heidelberg, 2001).
18. V. GARCÍA BROSA, C. BERNAL and P. FRONTINI, *Eng. Fract. Mech.* **62** (1999) 231.
19. W. GRELLMANN, S. SEIDLER, K. JUNG and I. KOTTER, *J. Appl. Polym. Sci.* **79** (2001) 2317.
20. Y. HAN, R. LACH and W. GRELLMANN, *ibid.* **79** (2001) 9.
21. K. KNOLL and N. NIEßNER, *Macromol. Symp.* **232** (1998) 231.
22. W. GRELLMANN, S. SEIDLER and W. HESSE, in "Deformation and Fracture Behaviour of Polymers," edited by W. Grellmann and S. Seidler (Springer, Berlin Heidelberg, 2001) p. 71.
23. S. SEIDLER and W. GRELLMANN, in "Deformation and Fracture Behaviour of Polymers," edited by W. Grellmann and S. Seidler (Springer, Berlin Heidelberg, 2001) p. 87.
24. W. GRELLMANN and S. SEIDLER, in "Material Mechanics—Fracture Mechanics—Micro Mechanics," edited by T. Winkler and A. Schubert (DDP Goldenberg, Dresden, 1999) p. 336.
25. S. SEIDLER and W. GRELLMANN, *Intern. J. Fract., Lett. Fract. Micromech.* **96** (1999) L17.
26. W. GRELLMANN, R. LACH and S. SEIDLER, in "From Charpy to Present Impact Testing" (ESIS Publication 30), edited by A. Pineau and D. Francois (Elsevier Science, Amsterdam, 2002) p. 145.
27. R. ADHIKARI, R. LACH, G. H. MICHLER, R. WEIDISCH and K. KNOLL, *Macromol. Mater. Eng.* **288** (2003) 432.

28. W. GRELLMANN, S. SEIDLER and R. LACH, in "Proc. of 3rd International Conference on Mechanics of Time Dependent Materials" (University Erlangen-Nürnberg, Erlangen, 2000) p. 226.
29. W. GRELLMANN, in "Deformation and Fracture Behaviour of Polymers," edited by W. Grellmann and S. Seidler (Springer, Berlin Heidelberg, 2001) p. 3.
30. H. BLUMENAUER, E. SCHICK and R. ORTMANN, in "Bruchmechanische Werkstoffcharakterisierung," edited by H. Blumenauer (Deutscher Verlag für Grundstoffindustrie, Leipzig, 1991) p. 31.
31. W. GRELLMANN and R. LACH, *Appl. Macromol. Chem. Phys.* **253** (1997) 27.
32. S. WU, *Polymer* **26** (1985) 1855.
33. A. MARGOLINA, *Polym. Commun.* **31** (1990) 95.
34. G. H. MICHLER, *Acta Polymerica* **44** (1993) 113.
35. H. BEERBAUM and W. GRELLMANN, in "Fracture of Polymers, Composites and Adhesives" (ESIS Publication 27), edited by J. G. Williams and A. Pavan (Elsevier Science, Oxford, 2000) p. 163.
36. Y. HAN, R. LACH and W. GRELLMANN, *J. Appl. Polym. Sci.* **75** (2000) 1605.
37. W. GRELLMANN, unpublished results.
38. "Polymer Blends: Formulation and Performance," two-volume set, edited by D. R. Paul and C.B. Bucknall (Wiley, New York, 1999).
39. G. H. MICHLER, R. ADHIKARI, W. LEBEK, S. GOERLITZ, R. WEIDISCH and K. KNOLL, *J. Appl. Polym. Sci.* **85** (2002) 683.
40. R. ADHIKARI, R. GODEHARDT, W. LEBECK, R. WEIDISCH, G. H. MICHLER and K. KNOLL, *J. Macromol. Sci., Phys.* B **40** (2001) 833.

Received 10 February
and accepted 7 October 2003